数理解析研究所講究録
1141 巻 2000 年 115-127

Asymptotic regimes in turbulence under simple shear: linear theory

K. N. Beronov and Y. Kaneda

Dept. Computational Science and Engineering,
Graduate School of Engineering, Nagoya Univ.

1 Introduction

This work is part of a project on modeling of global–scale flows.Wind shear, both vertical and horizontal, is a dominant and long lasting feature of atmospheric dynamics. In the geophysical context it is customary to study the effect of shear only in combination with stratification and sometimes also with the Coriolis force added. In the engineering literature, on the other hand, the study of sheared turbulence statistic is always related to modeling of turbulent boundary layers. Here, the effect of linear velocity shear on small–scale turbulent velocity fluctuations is studied taken in isolation, and the initial state of turbulence is assumed homogeneous. This setup is standard in turbulence theory and its results define part of the frame for parametric study of the combined effect of the three mentioned large-scale effects on geophysical turbulence.

Even after the dramatic simplifications adopted here in order to make direct use of the classical linear results known as Rapid distortion theory (*RDT*) for simple shear flow, there remain aspects in which the parametric region covered by the available theory is incomplete. An attempt is made here to describe two of these aspects: the effect of viscous dissipation, and the application of *RDT* at large times. Although some numerical results have suggested that *RDT* for simple shear (*SSRDT*) can produce rather satisfactory description of turbulence over extended periods, it seems to be generally accepted, and indicated by the term "rapid", that the application of linear theory is only justified over short intervals. When shear is sufficiently stronger than nonlinearty, however, times referred as "short" in the latter sense are so "extended" that shear is able to determine completely most of the qualitative features of distorted turbulence. As a result, a universal structure emerges from a variety of initial conditions. Counter to the general belief, linear theory can give an adequate description of weak turbulence at long times. This description is simpler and theoretically richer than the short-time applications provided by all but one of the references on *SSRDT*.

Asymptotics of single-point velocity correlations are given in [11] for the inviscid case. Here, two-point velocity correlations as well as vorticity correlations are integrated up to large times; their transients and final asymptotes are described. The effect of viscosity is added; it is found to induce some universality in the long–time behaviour, independent of the value of viscosity but different from the inviscid regime which appears as a singular limit.

Computation of correlations by *SSRDT* is feasible up to very large times, while all present laboratory experiments and *DNS* are confined to nondimensional times $\tau = \mathrm{O}(10)$. Here, good agreement in the evolution of important statistics is found between experiments and linear theory. This shows that judicious use of *SSRDT* presents a valuable prognostic model.

2 Formulation

Basic non-dimensional variables are the Eulerian coordinates $\boldsymbol{x} = L(x_1, x_2, x_3)$, time $\tau = tS$, mean flow velocity $\boldsymbol{U} = S(x_3, 0, 0)$, mean flow vorticity $\boldsymbol{\Omega} = S(0, 1, 0)$. To fix time and length–scales, choose the shear stength $S=1$, and turbulence integral length–scale$L=\mathrm{O}(1)$ $\ll$ mean flow length–scale. The relative importance of viscosity is expressed by the Townsend parameter $N = 4\nu/L^2S$. Systematic study of the N–dependence is one of the subjects here.

The evolution for single modes with respect to Lagrangian wave–vectors $\boldsymbol{k} = k\boldsymbol{q}$ is easily expressed in analytic form; in the inviscid case it depends only on the direction $\boldsymbol{q}$ ($\|\boldsymbol{q}\| = 1$). While the Lagrangian wave–vector is constant in such a formulation, the Eulerian wave–vector $\boldsymbol{\kappa}$ is time–dependent: $\boldsymbol{\kappa}(0) = \boldsymbol{k}$, $\mathrm{d}\boldsymbol{\kappa}/\mathrm{d}\tau = -\boldsymbol{S}\cdot\boldsymbol{\kappa}$. The evolution of each mode's velocity follows $\widehat{\boldsymbol{u}}(\boldsymbol{\kappa},\tau) = D\,\boldsymbol{A}(\boldsymbol{q},\tau)\cdot\widehat{\boldsymbol{u}}(\boldsymbol{\kappa},0)$, where the viscous damping factor $D = \exp\left(-\nu k^2\tau A_0(\boldsymbol{q},\tau)\right)$ is a scalar, and the inviscid Green's function $\boldsymbol{A}$ is a matrix with only few time–dependent entries, $A_j(\boldsymbol{q},\tau)$, $j=1,2,3$. All A_j are known analytically [16, 11].

The initial ($\tau = 0$) turbulence is assumed isotropic, with energy spectrum $E_{ij}(k,0) = \mathrm{e}^{-\Psi(Lk)}\,(Lk)^{2n}\,L^3\big/4\pi c_{n+1}^2$, $\forall i,j = 1,2,3$, with $1 \le n \le 2$ and $c_n^2 = \int_0^\infty \mathrm{d}k \mathrm{e}^{-\Psi(k)}k^{2n}$. Here $E_{ij}(k,\boldsymbol{q},\tau) = \langle\widehat{u_i}(\boldsymbol{k},\tau)\,\widehat{u_j}^*(\boldsymbol{k},\tau)\rangle$ denotes the spectral tensor corresponding to the ensemble average of the $\boldsymbol{k}$ mode at time τ. At $\tau>0$ this is no longer a multiple of the identity matrix. The transfer of energy in the case of simple shear is characterized by the magnitude of E_{13} relative to the energy E_{11} in the dominant streamwise velocity component. The traditional subject of RDT has been the single-time, single-point velocity correlation tensor $E_{ij}(\tau) = \int_0^\infty \mathrm{d}k \int \mathrm{d}\boldsymbol{q} E_{ij}(k,\boldsymbol{q},\tau)$. Here we conisder also the simplest two-point velocity correlations $E_{ij}^{[m]}(\tau) = \int_0^\infty \mathrm{d}k \int_{q_m=0} \mathrm{d}\boldsymbol{q} E_{ij}(k,\boldsymbol{q},\tau) = \int_{-\infty}^{+\infty}\big\langle u_i(\boldsymbol{x},\tau)\,u_j(\boldsymbol{x}+s\boldsymbol{\eta}_m,\tau)\big\rangle\,\mathrm{d}s$, where $\boldsymbol{\eta}_m$ denotes a unit vector in the x_m coordinate direction. Unlike any previous $SSRDT$ works, the evolution of the vorticity correlation tensor $\boldsymbol{\mathcal{E}}(k,\boldsymbol{q},\tau) = -\boldsymbol{\Omega}\cdot\boldsymbol{E}\cdot\boldsymbol{\Omega}$ is also considered. Here $\Omega_{i,j} = \varepsilon_{i,j,m}\,(q_j - \delta_{j,3}q_1\tau)$ and ε is the alternating tensor. Discussion of vorticity is confinded only to the single-point correlation $\boldsymbol{\mathcal{E}}(\tau)$, although $\boldsymbol{\mathcal{E}}^{\square}$ (τ) are easier to compute.

Compared to Townsend's seminal work [15], the condition $n = 2$ is relaxed, but the form $\Psi(k) = \exp\left(-k^2/2\right)$ of high-wavenumber decay will be still assumed. The reason is that this form emerges in the long–time limit from *any* initial spectrum with monotonous $\Psi(k)$. All statistics are conveniently calculated in terms of $\boldsymbol{B}(\boldsymbol{q},\tau) = \boldsymbol{A}\cdot\boldsymbol{E}\cdot\boldsymbol{A}^{\mathrm{T}}$ and $D_n(N,\boldsymbol{q},\tau) = \int_0^\infty \mathrm{d}k\; D(\nu,\boldsymbol{q},\tau)\;\mathrm{e}^{-(kL)^2/2}(Lk)^{2n}L^3\big/4\pi c_{n+1}^2 = \big(1 + N\tau A_0(\boldsymbol{q},\tau)\big)^{-(n+1/2)}$.

The evolution only of single-time statistics is considered. No study of the effect of helicity or anisotropy is attempted. It would be difficult to compare such quantities with readily available experimental data. The main goal of the presented investigation is to identify simple and universal features of the evolution of sheared turbulence; for this reason the attention is concentrated on quantities involving much spatial averaging, measured at late times, so as to reduce as much as possible the inflience of initial conditions.

3 Evaluation methods

This work consists of three parts: (1) numerical computation of correlations, (2) comparison with experimental data for as long intervals of time as possible, and (3) asymptotic analysis of the long–time limit to explain the time–scalings observed from the numerical results, typically at much longer times. One of the sections is devoted to the presentation and

discussion of results obtained in each of these parts. The required background information for all of them is summarized here.

Choice of numerical method The natural method for calculating single-time statistics from *DNS* data is to take averages over the fixed Fourier–space grid. This is simple and fast, but is found to be appropriate only for $\tau < 10^1$, which is also the time range of presently known *DNS*. (It might be speculated that *RDT* is not applicable even for τ of that order, but this can only be judged from a comparison between experimental data and precise computations from the theory.) The alternative method is to integrate by an adaptive numerical method the analytic formulae of *SSRDT* (for single-point velocity moments, cf. [1, 2, 15]). Using a standard Gaussian adaptive quadrature, it was possible to obtain reliable results at least up to $\tau = \mathrm{O}(10^3)$. It is easy to compute two-point statistics up to $\tau \geq 10^4$, because the integral in then one-dimensional.

The reason for the stringent limitation on τ in the simple shear case is that with time the total energy concentrates into an $\mathrm{O}(\tau^{-1})$ neighborhood of the resonant surface $q_1 = 0$. Modes in this neighborhood will be called *slow modes*, because the time variation of their Eulerian wave–vector is so slow that $\kappa_3 = q_3 - \tau q_1$ remains $\mathrm{O}(1)$ while for *general modes* is is $\mathrm{O}(\tau)$ at $\tau \gg 1$. The slow modes cannot be represented adequately by a discrete wavenumber grid for times $\tau > (\Delta k)^{-1}$ where Δk is a representative step between neighboring mesh points. Refinement of the grid soon becomes overly expensive.

Presentation of *SSRDT* numerics While Townsend [15] has plotted the evaluation of his single-point formulate for $N = 0, 0.2, 0.4, 0.8$, a logarithmic step $N = 0$, 10^{-3}, 10^{-2}, 10^{-1}, 1 is chosen here to demonstrate time-scaling on *log–log* plots. The same N values and line styles are used for all kinds of correlations predicted by *SSRDT*. Experimental data are shown by discrete symbols.

SSRDT curves are rescaled to fit best the magnitude of experimental points when the latter have unknown normalization. In all cases, averaged initial conditions in the experiments are different from the isotropic spectrum assumed in the *SSRDT* presented here. The only freedom allowd to improve agreement in the presented plots is a shift in the origin of the *RDT* curve. This correction is always $\tau_0 \leq \mathrm{O}(1)$. The obtained improvement has a physical meaning: Strong initial anisotropy not related to the mean flow shear is first reduced, during an initial transient, after which the evolution is close to the *SSRDT* prediction.

Experimental data chosen for comparison It is meaningless to compare *RDT* predictions with data from experiments in which nonlinearity or other effects not accounted in the theory make a dominant contribution. Comparison is naturally made in terms of the quantities presented in the respective journal references. *SSRDT* values are derived from numerically computed time sequences for the velocity and vorticity correlation tensors.

From all references on *DNS* of sheared turbulence, only one is chosen [8], because it presents a dynamics definitely dominated by the *SSRDT* operator, and also because it is a realtively long run with a method and resolution that assure precision of results. The main topic of that reference is to quantify the evolution of *componental anisotropy* in the turbulent velocity and vorticity [8], rather than the classical plots of turbulent energy growth and evolution of turbulent lengthscales found in most references.

Two reports of laboratory experiment are chosen for comparison — one set of wind tunnel measurements [5] and another set from a water channel [9]. Both reports provide sufficiently detailed documentation, reasonably uniform and strong shear levels, and data that are qualitatively compatible with *SSRDT*. Other recent experiments obtain even stronger shear rates and maximum τ, but exhibit different time scalings (quadratic or exponential — the discussion [14, 9] on which is the correct one remains so far left open) for the total energy than predicted by *SSRDT*. The most plausible reason is that the experimental setup in those cases generates strong nonlinearty which can by itself account for the change in time scaling (see also the concluding section).

Nature of long–time asymptotics The slow modes grow longer and decay more slowly than general modes. For correlations of interest, this difference scales as integer powers of τ, so in most cases the contribution by slow modes completely determines the leading-order term in $\tau \gg 1$ expansions. Whenever necessary, the contribution by general modes is computed separately. This general procedure was first applied in [11] to analyse the inviscid long–time limit of single-point velocity correlations. While power laws are readily deduced from the asymptotic forms of $A_j(\tau)$, $j = 0, \ldots 3$, the coefficients of the leading-order terms result from quadratures, some of which have to be evaluated numerically.

4 Comparison with experiments

Integral length–scale It is known that the streamwise integral length–scale of turbulence, $L_{11}^{[1]}(\tau) = E_{11}^{[m]}/E_{11}$ up to a normalization constant, grows with time in a shearing mean flow. The *SSRDT* prediction at $\tau \gg 1$ is for linear growth, for any value of N. This contradicts no experimental data known to us. A comparison with both wind tunnel and water channel data is shown in Fig. 1. All *SSRDT* cirves are shifted right by about $\tau_0 = 2$.

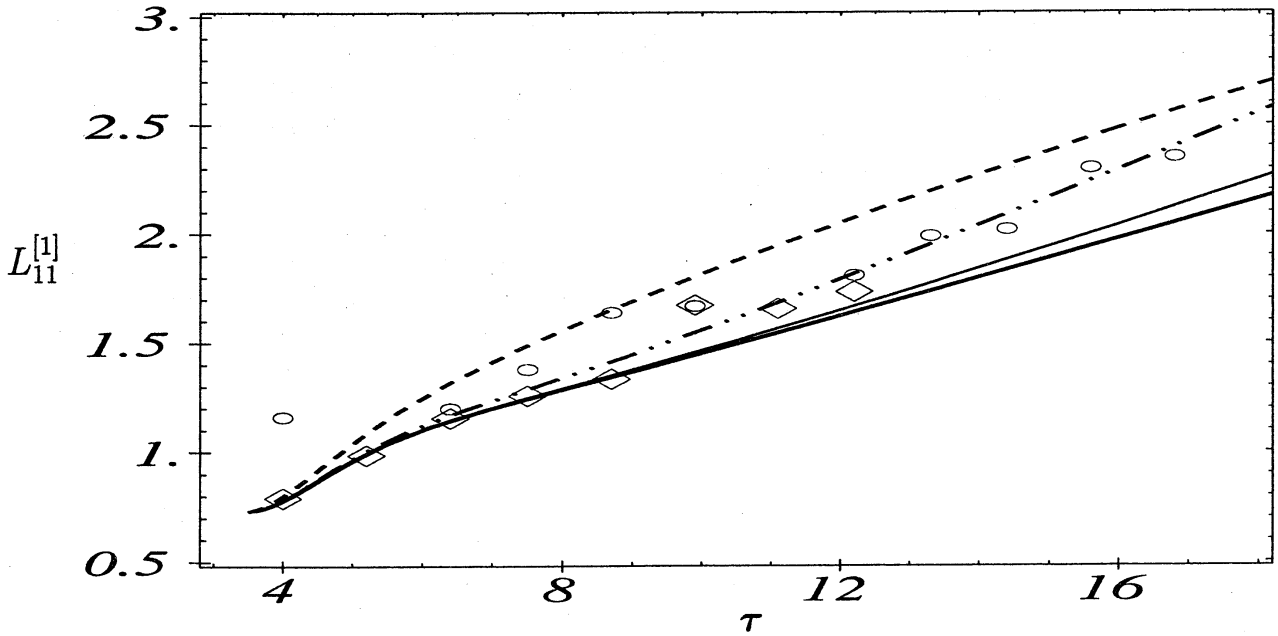

Figure 1: Integral length–scale evolution. Wind tunnel (◇) and water channel (o) data and numerical *SSRDT* (from topmost, solid curve downward: $N = 0$, 10^{-3}, 10^{-2}, 10^{-1}).

Eddy viscosities producing $N = \mathrm{O}(10^{-2})$ are seen as best candidates for a viscous *SSRDT* fit. (The actual viscosities and corresponding N are different in the two experiments.) Ignoring the scatter and wavyness of experimental data and the unavoidable deviations during the initial transient, the agreement is rather good. It seems that the experiments confirm the tendency to first follow the inviscid curve and later a viscous curve that tends to an N-invariant curve at $\tau \gg 1$, which is approximately illustrated by the topmost ($N = 0.1$) curve in the figure. This lends support to Townsend's [16] idea of modeling nonlinearty as eddy viscosity, and also emphasizes the need for a detailed viscous *SSRDT* at large τ.

Taylor microscale In isotropic turbulence, the microscale λ is defined by $\lambda^2 = 15\nu\,(E_{11})\,\varepsilon^{-1} = \left(5\sum_j E_{jj}\right)\left(\sum_j \mathcal{E}_{jj}\right)^{-1}$, where ε is the energy dissipation rate. The first form is used in experimental estimates, while the second form, a ratio between total turbulent energy and enstrophy, is readily evaluated from numerical data, either from *DNS* or *RDT*. For developed turbulence, λ is an intrinsic length–scale, characteristic of inertial-range structures much smaller than the energy containing eddies and thus dominated by nonlinear transfer rather than strongly influenced by the forcing mechanism.

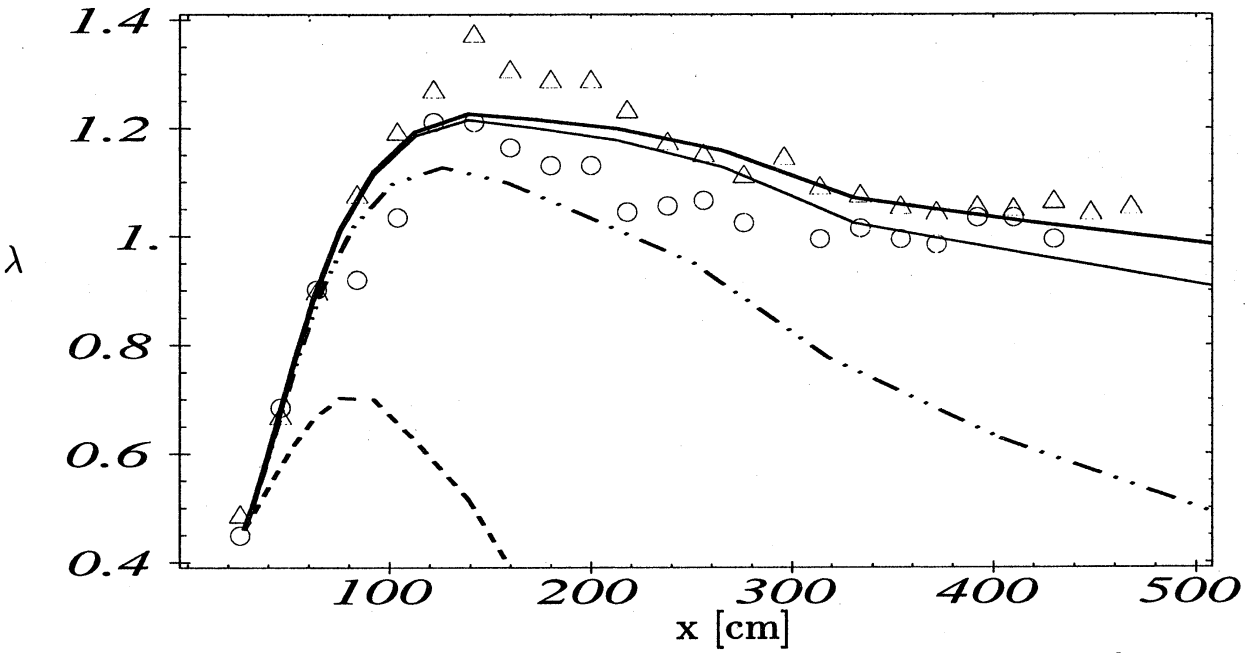

Figure 2: Taylor microscale evolution: Fitting two water channel data sets by numerical *SSRDT* results. From topmost (solid) curve downward: $N = 0$, 10^{-3}, 10^{-2}, 10^{-1}.

In sheared turbulence, the linear operator due to the mean flow generates small scales; when shear is stronger than nonlinearty, is its effect dominates up to scales much smaller than the energy containing ones. Comparison of $\lambda(\tau)$ obtained from the present *SSRDT* calculations with experimental data obtained pin a water channel is given in Fig. 2. The last data points in both experimental runs shown correspond approximately to $\tau = 20$. Noting that curves are spaced logarithmically with respect to the parameter N, and that the laboratory flow is far from the idealized conditions assumed in the *RDT* computation, the agreement at small N is rather good.

Componental anisotropy of velocity and vorticity The anisotropy tensor $b_{ja}[i]$ and Lumley's scalar measure of anisotropy $II^b[\boldsymbol{a}]$ are calculated for any (ensemble of) vector fields $\boldsymbol{a}$ from the single-point correlation tensor $E_{ij}(\boldsymbol{a})=\langle a_i\, a_j\rangle$ as follows:

$$II^b[\boldsymbol{a}] = \frac{1}{2}\sum_{i=1}^{3}\sum_{j=1}^{3}\left(b_{ij}[\boldsymbol{a}]\right)^2, \qquad b_{ij}[\boldsymbol{a}] = b_{ji}[\boldsymbol{a}] = E_{ij}\left(\sum_{n=1}^{3} E_{nn}\right)^{-1} - \frac{1}{3}\,\delta_{ij}$$

It can be shown that $-1/3 < b_{jj}[\boldsymbol{a}] < 2/3$, $-1/2 < b_{j+1,j-1}[\boldsymbol{a}] < 1/2$, and $0 \le 3II^b[\boldsymbol{a}] \le 1$. All vanish for perfect isotropic $\boldsymbol{a}$. Fields with single dominant component give $3II^b[\boldsymbol{a}] = 1$, while "two-component" fields in which the ratio of the dominant components stablizes with time give $3II^b[\boldsymbol{a}] \to$ const. with $0 <$ const. < 1. In simple shear, the turbulent velocity and vorticity tend to become at large τ respectively single-component is two-component.

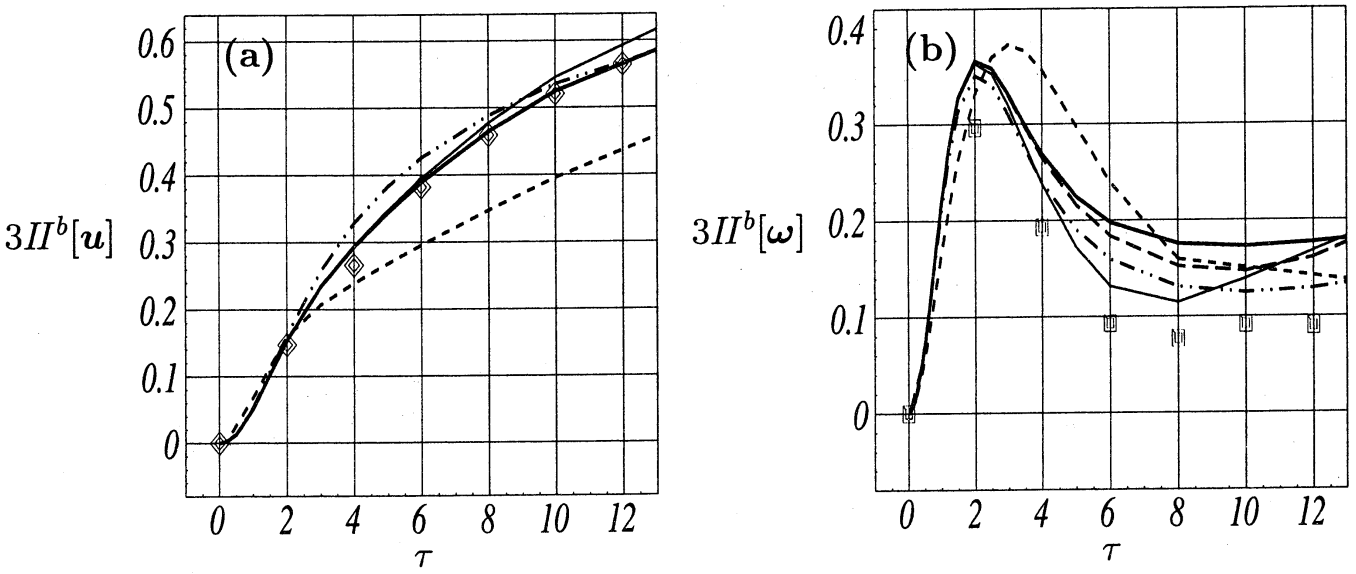

Figure 3: Evolution of the 2nd invariant of the anisotropy tensor for (a) the velocity and (b) the vorticity field. Symbols denote *DNS* data [8]. Lines connect *SSRDT* data sequences for $N=0$ (————), 10^{-3} (——), 10^{-2} (—·—), 10^{-1} (— —), 1 (- - -).

In Fig. 3 the data for the velocity $\boldsymbol{a}=\boldsymbol{u}$ and vorticity $\boldsymbol{a}=\boldsymbol{\omega}$ from *DNS* spatial averages [8] and from the present *SSRDT* computation of ensemble averages are compared. The initial spectrum for the *DNS* is nearly isotropic but with much slowlier decay at large wavenumbers, which may explain the larger difference between theory and *DNS* in the vorticity data (b). The implied ratio of components in the *DNS* data is closer to 1 than both viscous and inviscid *SSRDT* limits, but the viscous limit (cf. $N=0.1$ and 1 curves) is a better approximation. In any case, the $N \ll 1$ curves of *SSRDT* agree with the single-realization *DNS* data over both the transient and the long–time τ-ranges.

Vorticity anisotropy is seen to be much more sensitive than velocity anisotropy to forcing parameters like initial spectrum and viscosity, and single components $b_{ij}[\boldsymbol{\omega}]$, shown in Fig. 4, are more sensitive than the $II^b[\boldsymbol{\omega}]$ square–mean. Best approximation obtains for $N=\mathrm{O}(10^{-2})$; the numerical viscosity used in that *DNS* is of that order, as well.

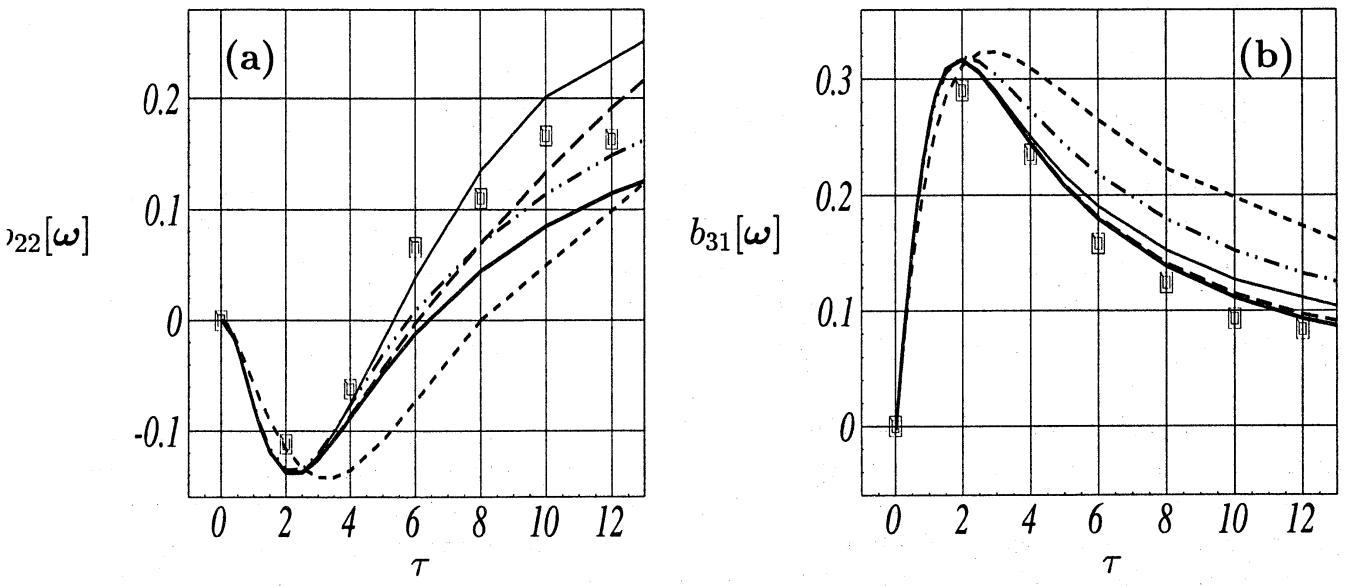

Figure 4: *SSRDT* for vorticity anisotropy tensor components with asymptotes qualitatively independent on viscosity. Symbols denote *DNS* data [8]. Lines connect *SSRDT* data sequences for $N=0$ (————), 10^{-3} (— —), 10^{-2} (——), 10^{-1} (—·—), 1 (- - -).

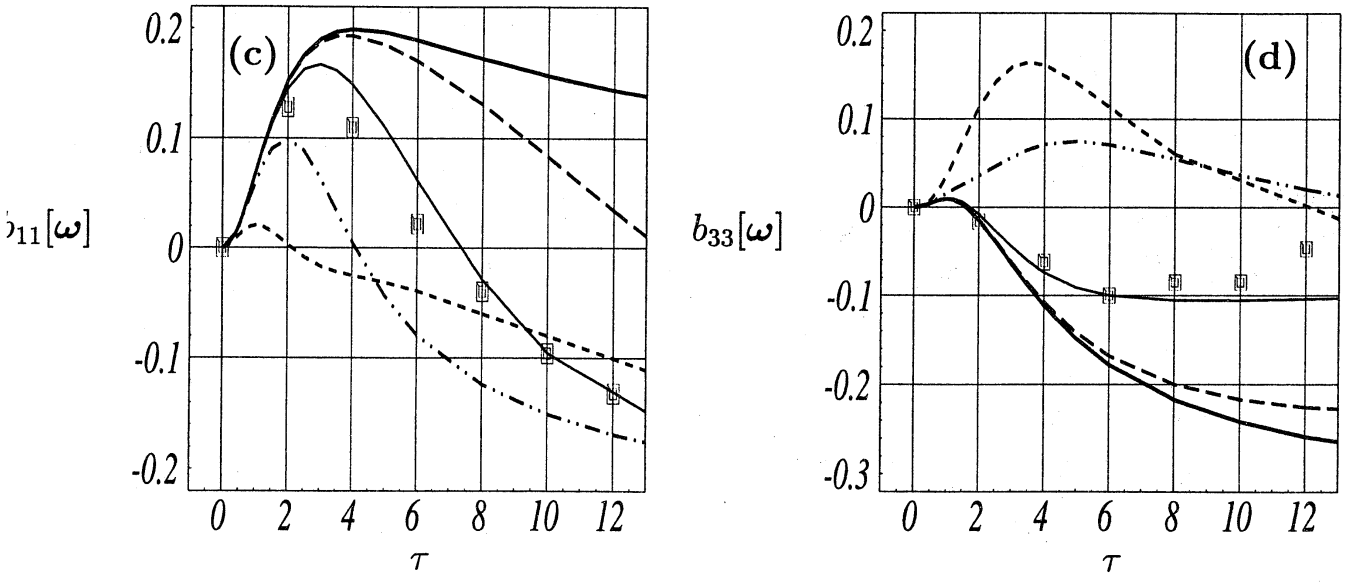

Figure 4: (continued) *SSRDT* for vorticity anisotropy components sensitive to N.

The particularly strong dependence of $b_{11}[\omega]$ and $b_{33}[\omega]$ on N is related to the finding from long–time *SSRDT* (numerically and analytically, see further below) that the second dominant component, beside ω_2, is different in the inviscid and the viscous case.

5 Transients and long–time universality

The universality of the viscous long–time regime consists in the independence on N and difference from the $N = 0$ case of the asymptotics of *ratios* of correlations, such as the anisotropy measures shown in the previous section or the simple ratios E_{ij}/E_{11} which were plotted, although only for $\tau < 10$, already by Townsend [16]. The present section is to demonstrate that universality and the power laws governing long–time *SSRDT* evolution.

Velocity correlations The ratio of main practical interest, E_{13}/E_{11}, characterized energy transfer toward the streamwise velocity component which becomes so much dominant at late times that E_{11} gives effectively the total turbulent energy. In practice, that this ratio tends to a constant which sttrongly fluctuates from one experiment to the other, despite numerous efforts to find the "true" value. In *SSRDT*, there is no nonlinear term to feed back into E_{33}, which constantly looses energy, mainly to E_{11}; this is reflected by $\tau \gg 1$ scaling predictions $\sim \tau^{-1}$ and $\sim \tau^{1}$ respectively. As a consequence *SSRDT* predicts $E_{13} = \mathrm{O}(1)$. This scaling is illustrated in Fig. 5(a). With only a slightly different constant prefactor the same power law asymptotics hold for the corresponding ratio of a typical two-point correlation tensor, like $E_{ij}^{[3]}$ shown in Fig. 5(b). It is noted that the viscous asymptote has the same power law but different prefactor than the inviscid one, both being O (1). The same qualitative observation holds true for all other ratios of single-point and of *typical* two-point correlations.

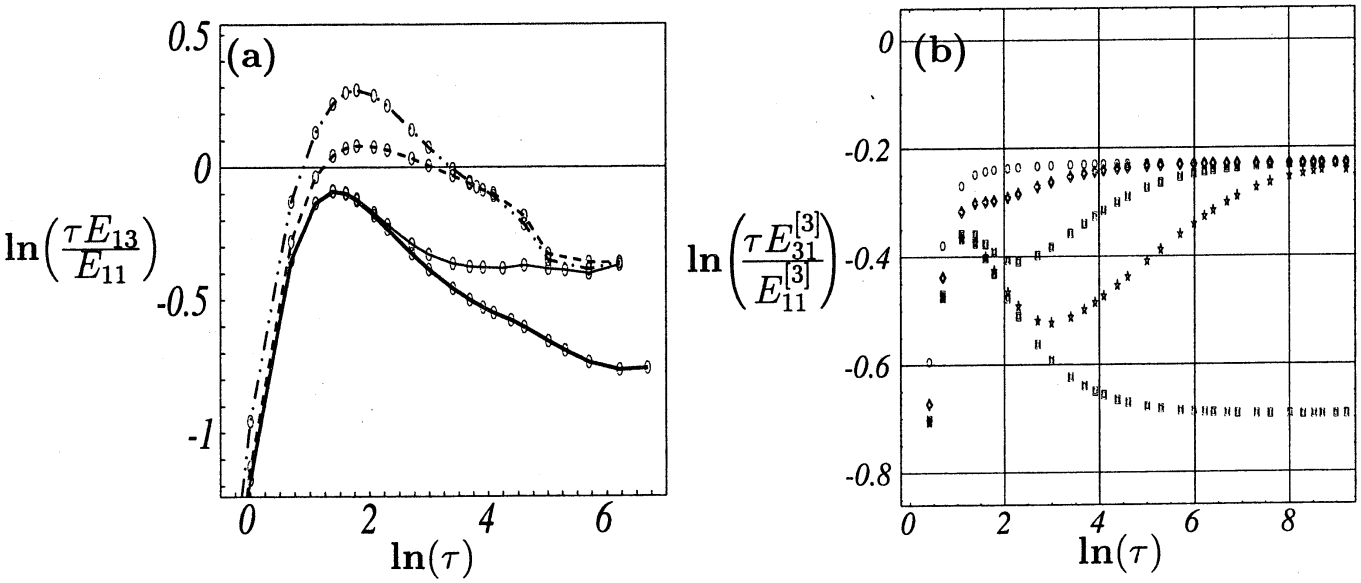

Figure 5: Compensated (a) single-point and (b) two-point ratios of Reynolds stress to streamwise (dominant) componental energy. From lowest curve up, (b): $N = 0$, 10^{-3}, 10^{-2}, 10^{-1}, 1; (a): 10^{-3} not shown. Aymptotes τ const. have const. < 1 closer to 1 in the viscous case.

Precise knowledge of the *RDT* scaling laws is nevertheless necessary in modeling the actual energy transfer rate. The second ingredient in a model, which will not be discussed here, must be the nonlinear transfer rate toward E_{33}. Balance of the two asymptotic rates would yield an estimate of the true E_{33}/E_{11} ratio, which would clearly depend on the turbulent Reynolds number. Only the limit when the latter is zero is considered here. The important result is the independence on the other parameter, $N>0$, of the asymptotic ratios in *SSRDT*. What does depend on N is the time it takes for ratios of correlations to depart from the corresponding inviscid curves and to approach the viscous ones. As noted earlier [11] for the $N=0$ case, the time taken by compensated ratios to approach a constant (on Fig. 5 this means to a horizontal line) depends on the indices i, j of E_{ij}. Now the effect of $N>0$ on each separate ratio can be seen — both the departure from the $N=0$ curve and convergence with the universal viscous asymptote at times $O(N^{-1})$.

Vorticity correlations The dominant turbulent velocity component aligns at $\tau \gg 1$ with the mean flow velocity. Similarly, *SSRDT* predicts and *DNS* confirm that, at $\tau \gg 1$ the dominant turbulent vorticity component is the one aligned with the mean flow vorticity. The evolution of the corresponding single-point correlation $\mathcal{E}_{22}(\tau)$ is shown in (6).

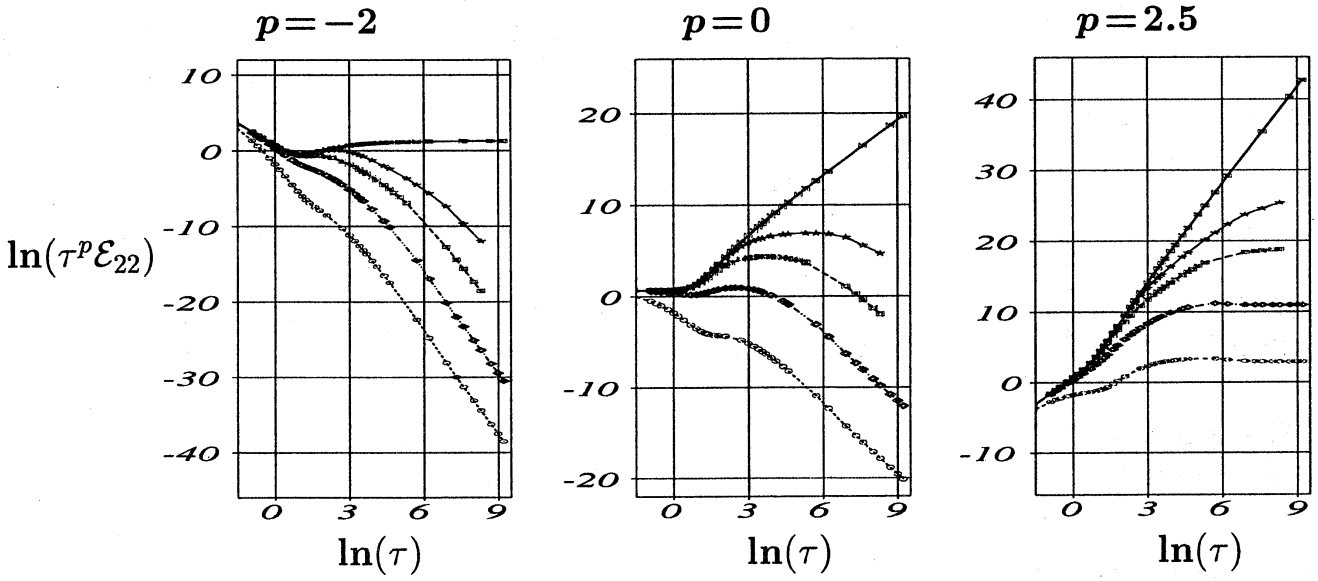

Figure 6: Spanwise "enstrophy tensor" compensated by different power-laws, $\mathcal{E}_{22}(\tau)\,\tau^{-p}$. From topmost curve downward, on each plot, $N=0$, 10^{-3}, 10^{-2}, 10^{-1}, 1.

The left plot (a) shows the inviscid asymptote as a horizontal line. The right plot (c) shows the same data compensated differently, so that viscous asymptotes appear as horizontal lines. The middle plot (b) shows a transient, over times $O(N^{-1})$, which has not been identified previously in the literature. Although the average relative magnitudes of vorticity components in that regime are as in the final viscous decay regime, enstrophy does not decay over long time spans. This regime can be of substantial importance in stability analysis of sheared flows; its appearance at small N is explained in the following section.

The structure of the vorticity field changes dramatically in time. Most currently published *DNS* emphasize the first transient, during which an initially nearly isotropic field is stretched by the mean shear and strong, elongated, nearly *streamwise vortices* come to dominate the ω field. In some publications however (see e.g. [10]), it is shown that at later times the

typical vorticity lines are predominantly oriented in the *spanwise* direction. This turning of the vorticity field is captured by *SSRDT*. It can be seen in the evolution of correlation ratios involving $\mathcal{E}_{22}$. As seen from Fig. 7 and supported analytically in the next section, there is always one more component that remains comparable to, albeit smaller than ω_2 (this trend toward a "two-component field" has already been noted [8] form the relatively short-time data of a strong-shear *DNS*). The inviscid vorticity asymptote (bold line) scales differently than the viscous one (all other lines). At $\tau \gg 1$, *SSRDT* predicts $\mathcal{E}_{11}/\mathcal{E}_{22} = \mathrm{O}(1)$ and $\mathcal{E}_{33}/\mathcal{E}_{22} \to 0$ if $N=0$, but $\mathcal{E}_{11}/\mathcal{E}_{22} \to 0$ and $\mathcal{E}_{33}/\mathcal{E}_{22} = \mathrm{O}(1)$ if $N>0$.

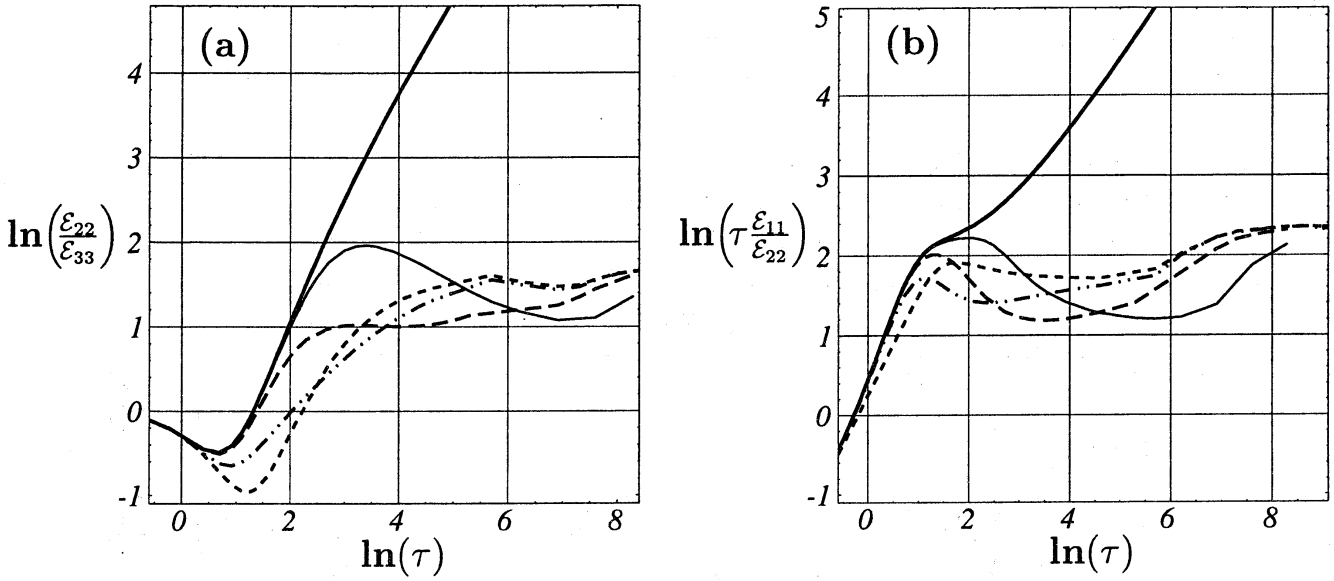

Figure 7: Componental entsrophy ratios involving the dominant moment $\mathcal{E}_{22}$. Bold lines: $N=0$. All other lines start to deviate from the $N=0$ ones at $\tau \propto N^{-1} = 1,\ 10^1,\ 10^2,\ 10^3$.

The approximate asymptotic values $\mathcal{E}_{11}/\mathcal{E}_{22} \to 0.52$ if $N=0$ and $\mathcal{E}_{33}/\mathcal{E}_{22} \to 0.85$ if $N>0$ can be evaluated from the extension of Fig. 3(a,c) to much larger τ, shown in Fig. 8.

6 Asymptotic scalings

Some of the two-point velocity correlations considered here can be evaluated explicitly. In general, $E_{12}^{[m]} = E_{23}^{[m]} = 0$. The nontrivial streamwise correlations are $E_{11}^{[1]} = (1+N\tau)^{-(n+1)}(1+\tau^2)$, $E_{22}^{[1]} = E_{33}^{[1]} = (1+N\tau)^{-(n+1)}$, $-E_{31}^{[1]} = (1+N\tau)^{-(n+1)}\,\tau$; they are growing faster with τ than their $E_{ij}^{[2]}$ or $E_{ij}^{[3]}$ counterparts. The spanwise correlations are untypical in many ways, e.g. they do not grow at all for $N=0$: $E_{22}^{[2]}=1$, $E_{11}^{[2]}=E_{33}^{[2]}=1/2$, $E_{31}^{[2]}=0$, and in the viscous case, $E_{11}^{[2]}=E_{22}^{[2]}/2$, $E_{22}^{[2]}=(1+\tau N/3)^{-(n+1)}$, $E_{31}^{[2]}=\mathrm{const.}E_{22}^{[2]}$, $\mathrm{const.}=\mathrm{O}(1)$. The nontrivial $E_{ij}^{[3]}$ and the single-point correlations require numerical evaluation, some of whose results were presented in the previous section. The long–time asymptotic limits, however, can be evaluated directly to leading order in τ. Some resulting quadratures are exact, e.g. $E_{11}^{[3]}=\tau\log(4)$, $E_{31}^{[3]}=\log(2)$, $E_{33}^{[3]}=\tau^{-2}/4$, and $E_{22}^{[3]}=1+(\pi/2)^2$ for $N=0$. The leading orders of those same moments follow from different expressions when $N>0$. Those give only the

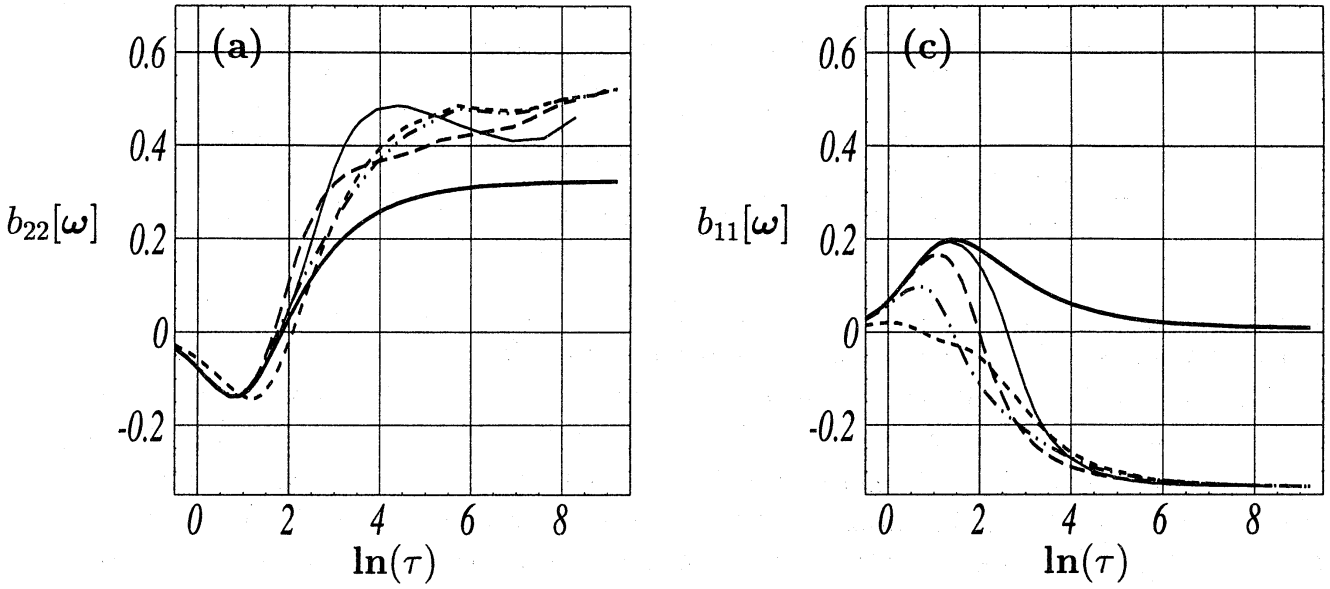

Figure 8: *SSRDT* for vorticity anisotropy tensor components $b_{ij}[\boldsymbol{\omega}]$.

slow mode contributions and have to be evaluated numerically:

$$N^2\tau^1 E_{11}^{[3]} \approx \pi^{-1}\int_{-\infty}^{\infty} \mathrm{d}\alpha\ (1+\alpha/3)^{-(n+1)}\ (\arctan(\alpha)/\alpha)^2$$

$$N^2\tau^2 E_{11}^{[3]} \approx \pi^{-1}\int_{-\infty}^{\infty} \mathrm{d}\alpha\ (1+\alpha/3)^{-(n+1)}\ \arctan(\alpha)/\left(\alpha\left(1+\alpha^2\right)\right)$$

$$N^2\tau^3 E_{13}^{[3]} \approx \pi^{-1}\int_{-\infty}^{\infty} \mathrm{d}\alpha\ (1+\alpha/3)^{-(n+1)}\ \left(1+\alpha^2\right)^{-2}$$

$$N^2\tau^3 E_{12}^{[2]} \approx \pi^{-1}\int_{-\infty}^{\infty} \mathrm{d}\alpha\ (1+\alpha/3)^{-(n+1)}\ \left(\arctan(\alpha)+\alpha/\left(1+\alpha^2\right)\right)^2$$

Numerical investigation of the n-dependence shows that all constants except the one pertaining to $E_{22}^{[3]}$ are nearly constant for $1/2<n\leq 2$. In Townsend's [16] case $n=2$, the respective values are 0.580, 0.462, 0.3905, 1.074.

The inviscid vorticity asymptotics are more complicated because in many cases the contribution by slow modes is not dominant, unlike all velocity correlations except $E_{22}^{[3]}$ and all

Table 1: Asymptotic *SSRDT* scalings of single-point and two-point velocity correlations.

m	N	$E_{11}^{[m]}$	$E_{22}^{[m]}$	$E_{33}^{[m]}$	$E_{31}^{[m]}$	$L_1^{[m]}$	$L_2^{[m]}$	$L_3^{[m]}$
0	$=0$	1	0	-1	0			
0	>0	$-n-1/2$	$-n-3/2$	$-n-5/2$	$-n-3/2$			
1	$=0$	2	0	0	1	1	0	1
1	>0	$-n+1$	$-n-1$	$-n-1$	$-n$	3/2	1/2	3/2
2	$=0$	0	0	0	0	-1	0	1
2	>0	$-n-1$	$-n-2$	$-n-1$		$-1/2$	$-1/2$	$-1/2$
3	$=0$	1	0	-1	0	0	0	0
3	>0	$-n$	$-n-2$	$-n-2$	$-n-1$	1/2	$-1/2$	1/2

Table 2: Asymptotic *SSRDT* scalings of single-point vorticity correlations.

	$\mathcal{E}_{11}$	$\mathcal{E}_{22}$	$\mathcal{E}_{33}$	$\mathcal{E}_{31}$	λ
inviscid	2	2	1	1	-1/4
transient	-1	0	0	-1	
viscous	$-(n+5/2)$	$-(n+3/2)$	$-(n+3/2)$	$-(n+5/2)$	1/2

cases with $N>0$. The inviscid asymptote $\mathcal{E}_{11}/\mathcal{E}_{22} = 3 - 32/\pi^2$ can be derived exactly. The transient viscous regime identified in the previous section from computations of $\mathcal{E}_{ij}(\tau)$ can be shown to result from a *subset of slow modes* as small as $\mathrm{O}(\tau^{-1})$, such that $N\tau A_0 \leq \mathrm{O}(1)$.

The exponents in the power laws $E_{ij}^{[m]}(\tau) \sim \tau^p$ of velocity correlations, which follow rigorously from *SSRDT* are summarized in Table 1, with $E_{ij}^{[0]} \equiv E_{ij}$ adopted for notational convenience. Since this information is all that is needed to know the scaling exponents of $L_j^{[m]}(\tau) = E_{jj}^{[m]} / E_{jj}$, those are also included in that table. The exponents for scaling laws of vorticity correlations are similarly collected in Table 2. The scaling of $\lambda = 5E/\mathcal{E}$ follows directly from information in these two tables, and is included along with vorticity scalings.

7 Conclusion

A complete long–time asymptotic linear theory of sheared weak turbulence is given for single-time single-point velocity and vorticity correlations. A new, viscous regime is described, which exhibits universal features, independent of the value of viscosity but different from the inviscid regime. Transition from inviscid to viscous asymptote occurs at times inversely proportional to viscosity; nearly inviscid transients can lead to large energy growth. This and other transients are described, which are more or less independent on initial conditions, unlike the initial transient on which previous *SSRDT* studies have focused. A new transient, within the viscous regime, is found important for vorticity statistics.

Successes of *SSRDT* in qualitatively predicting the long–time evolution of single-point and two-point statistics relates to various kinds of anisotropy measured in experiments: the establishment from different initial conditions of a universal sheared-tubulence regime dominated by streamwise streaks, the ordering between strain components, the change in the orientation of average vorticity from mostly streamwise to predominantly spanwise, the deviation of statistics from the inviscid *SSRDT* asymptote.

Failiures of *SSRDT* in qualitatively predicting long–time single-point, single–time statistics can be summarized as follows. Linear theory predicts linear growth of energy which is too slow in most cases, when quadratic or exponential growth is observed. Those scalings, however, can be accounted for by including nonlinear feedback in a simple modification of *SSRDT*, which will be presented elsewhere. Such a modification also aleviates the difference in long–time scaling exponents predicted by *SSRDT* for the different components of the single-point strain tensor. In experiments, these components tend to constant ratios within each realization, but the scatter between experiments is rather large and theory does not allow so far to expect any universality.

Successes of *SSRDT* in quantitatively predicting single–time statistics can be summarized as follows. All statistics related to velocity anisotropy in the reference *DNS* are are fitted fairly well by the corresponding inviscid *SSRDT* curves, as well as by $N = 10^{-2}$ which is of

the order of the relative value of viscosity in those simulations. The evolution of vorticity statistics is much more sensitive to the value of N; again, use of the value based on the "bare" viscosity in the simulation would give best results. Agreement with turbulence length–scales evolution data from laboratory experiments is as good as can be ever expected. Not only the integral length–scale but also the Taylor microscale data can be fitted and explained using *SSRDT*, because the linear shear dominates the generation of both large and fine scales.

References

[1] R. G. Deissler (1961), "Effects of inhomogeneity and of shear flow in weak turbulent fields", *Phys. Fluids* **4**, p.1187.

[2] R. G. Deissler (1965), "Velocity correlations in weak turbulent shear flow", *Phys. Fluids* **8**, p.391.

[3] R. G. Deissler (1975), "Comparison of theory and experiment for homogeneous turbulence with shear", *Phys. Fluids* **18**, p.1237.

[4] R. G. Deissler (1998), "Turbulent fluid motion.", Taylor & Francis, Philadelphia.

[5] V.G. Harris, J.A.H. Graham, and S. Corrsin (1977), "Further experiments on nearly homogeneous turbulent shear flow", *J. Fluid Mech.* **81**, p.657.

[6] U. Karnik and S. Tavoularis (1989), "Further experiments on the evolution of turbulent stresses and scales in uniformly sheared turbulence", *J. Fluid Mech.* **204**, p.457.

[7] S. Kida & M. Tanaka (1994), "Dynamics of vortical structures in a homogeneous shear flow", *J. Fluid Mech.* **274**, p.43.

[8] M. J. Lee, J. Kim, & P. Moin (1990), "Structure of turbulence at high shear rate", *J. Fluid Mech.* **216**, p.561.

[9] J.J. Rohr, E.C. Itsweire, K.N. Helland, and C.W. van Atta (1988), "An investigation of the growth of turbulence in a uniform-mean-shear flow", *J. Fluid Mech.* **187**, p.1.

[10] M. M. Rogers & P. Moin (1987), "The structure of the vorticity field in homogeneous turbulent flows", *J. Fluid Mech.* **176**, p.33.

[11] M. M. Rogers (1991), "The structure of a p@assive scalar field with a uniform mean gradient in rapidly sheared homogeneous turbulent flow", *Phys. Fluids A* **3**, p.144.

[12] Sahli and Cambon (1997), "An analysis of rotating shear flow using linear theory and DNS and LES results", *J. Fluid Mech.* **347**, p.171.

[13] A. M. Savill (1987), "Recent developments in rapid-distortion theory", *Ann. Rev. Fluid Mech.* **19**, p.531.

[14] S. Tavoularis (1985), "Asymptotic laws for transversely homogeneous turbulent shear flows", *Phys. Fluids* **28**, p.999.

[15] A. A. Townsend (1971), "Entrainment and the structure of turbulent flow", *J. Fluid Mech.* **41**, p.13.

[16] A. A. Townsend (1976), "The structure of turbulent shear flow", Cambridge Univ. Press.